Effect of Water on the Oxygen Barrier Properties of Poly(ethylene terephthalate) and Polylactide Films

Rafael Auras, Bruce Harte, Susan Selke

School of Packaging, Michigan State University, East Lansing, Michigan 48824-1223

Received 29 August 2003; accepted 4 December 2003

ABSTRACT: The aim of this work was to study the variations in the oxygen diffusion, solubility, and permeability coefficients of polylactide (PLA) films at different temperatures (5, 23, and 40°C) and water activities (0–0.9). The results were compared with the oxygen diffusion, solubility, and permeability coefficients obtained for poly(ethylene terephthalate) (PET) films under the same experimental conditions. The water sorption isotherm for PLA films was also determined. Diffusion coefficients were determined with the half-sorption time method. Also, a consistency test for continuous-flow permeability experimental data was run to obtain the diffusion coefficient with the lowest experimental error and to confirm that oxygen underwent Fickian diffusion in the PLA films. The permeability coefficients were obtained from steady-state permeability experiments. The results indicated that the PLA films absorbed very low amounts of water, and no significant variation of the absorbed water with the temperature was found. The oxygen permeability coefficients obtained for PLA films (2–12 $\times 10^{-18}$ kg m/m^2 s Pa) were higher than those obtained for PET films (1–6 $\times 10^{-19}$ kg m/m^2 s Pa) at different temperatures and water activities. Moreover, the permeability coefficients for PLA and PET films did not change significantly with changes in the water activity at temperatures lower than 23°C. © 2004 Wiley Periodicals, Inc. J Appl Polym Sci 92: 1790–1803, 2004

Key words: diffusion; barrier; biodegradable; films

INTRODUCTION

Polylactide (PLA) polymers derived from lactic acid (2-hydroxypropionic acid) are ready to be adopted as polymeric packaging materials. PLA has been widely studied for use in medical applications because of its bioresorbable and biocompatible properties in the human body.[1–7] Because of its higher cost, the initial focus of PLA as a packaging material has been in high-value films, rigid thermoforms, food and beverage containers, and coated papers. As modern and emerging technologies of producing PLA are lowering production costs,[8,9] PLA may have packaging applications for a broad array of products; moreover, new applications such as fibers are being pursued.[10]

The production of PLA presents numerous advantages: (1) it can be obtained from a renewable agricultural source (corn), (2) its production consumes quantities of carbon dioxide,[5] (3) it provides significant energy savings, (4) it can be recyclable and compostable,[9,11,12] (5) it can help improve farm economies, and (6) its physical and mechanical properties can be manipulated through the polymer architecture. Normally, PLA is fabricated through the polymerization of lactic acid monomer (LA), which is mostly produced through the carbohydrate fermentation of corn dextrose. Polymerization through lactide formation, patented by Cargill, Inc., in 1992,[9,13] is, by and large, the current method used for producing PLA. In this method, D-lactic acid, L-lactic acid, or a mixture of the two is prepolymerized to obtain an intermediate low-molecular-mass poly(lactic acid), which is then catalytically converted into a mixture of lactide stereoisomers. Lactide, the cyclic dimer of lactic acid, is formed by the condensation of two lactic acid molecules as follows: L-lactide (two L-lactic acid molecules), D-lactide (two D-lactic acid molecules), and *meso*-lactide (an L-lactic acid molecule and a D-lactic acid molecule; see Scheme 1). After vacuum distillation of the lactide, high-molecular-mass PLA with controlled optical purity and a constituent unit of —[OCH(CH_3)CO]— is formed through the ring-opening polymerization of the lactides.[9,14,15]

The properties of PLA, such as the melting point, mechanical strength, and crystallinity, are determined by the polymer architecture (i.e., the proportions of L-lactide, D-lactide, and *meso*-lactide) and the molecular mass. As for other plastics, the final user properties of PLA also depend on ordered structures, such as the crystalline thickness, crystallinity, spherulite size, morphology, and degree of chain orientation.[2,16] The proportions of D- and L-lactides determine the polymer morphology, and PLA can be produced that is totally amorphous or up to 40% crystalline. This results in PLA polymers with a wide range of hardness

Correspondence to: R. Auras (aurasraf@msu.edu).
Contract grant sponsor: Kraft Foods.

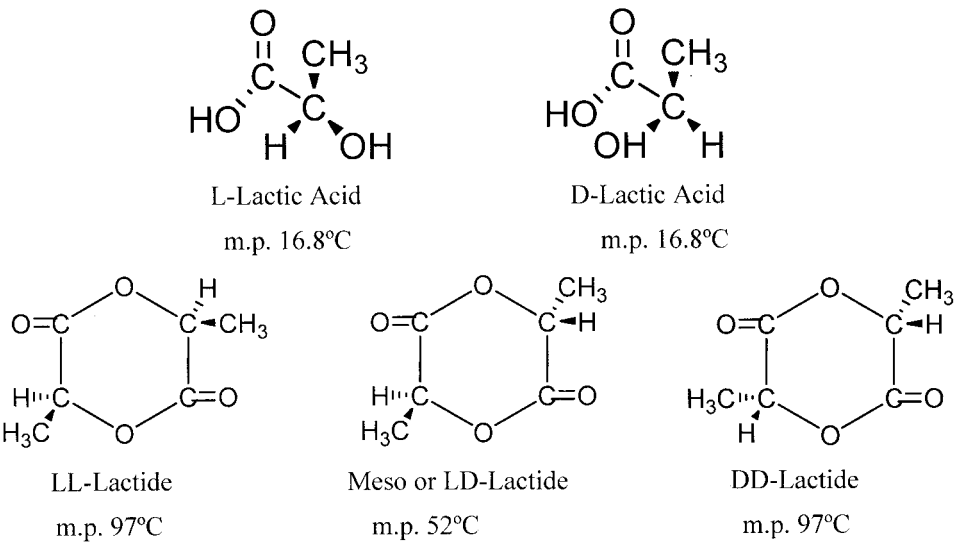

Scheme 1 Chemical structures of L-lactic acid, D-lactic acid, L-lactide, D-lactide, and *meso*-lactide.

and stiffness values. The glass-transition temperature (T_g) of PLA ranges from 50 to 80°C, whereas the melting temperature (T_m) ranges from 130 to 180°C.[2,16,17]

Early economic studies show that PLA is an economically feasible material for use as a packaging polymer.[8] Medical studies reported that the level of lactic acid that migrates to food from packaging containers is much lower than the amount of LA used in common food ingredients.[18] Therefore, polymers derived from lactic acid are good candidates for packaging applications.[2,5,17] Currently, PLA is being used as a food packaging polymer for short-shelf-life products with common applications, such as containers, drinking cups, sundae and salad cups, overwrap and lamination films, and blister packages.[19,20] In the next 5 years, PLA production and consumption are expected to increase.[8,19,21–25] Therefore, research into the variations of the physical, mechanical, and barrier properties of PLA polymers is necessary.

One of the main concerns for packaging polymers is their performance under real and differing environmental conditions (i.e., refrigerated, standard, and tropical conditions). Water–polymer interactions play a significant role in the general properties and aging of polymers. It is well known that the presence of water has a significant effect on the barrier and mechanical properties of most hydrophilic polymers. The presence of water or other small-molecular-mass compounds in the polymer matrix may change the way in which a gas or vapor is sorbed and diffused through the polymer.[26] For example, in the case of oxygen diffusion in hydrophilic polymers, the presence of water molecules that interact with the polymer matrix influences the mass-flow rate of the oxygen.[26,27] In the case of hydrophobic polymers or polymers free of hydrogen-bonding groups, such as poly(ethylene terephthalate) (PET) and PET-like polymers (e.g., PLA, because it has helix structures and bulky side chains[2]), the water equilibrium concentration under saturated conditions is typically lower than 2 wt %. Scheme 2 shows the constitutional units of PET and PLA polymers.

PET polymers absorb less than 60 ppm (w/w) water.[28] The room-temperature isotherm for PET films has been reported as a typical sigmoidal shape with water absorption lower than 1.0% at a water activity (A_w) higher than 0.9 [A_w is the ratio of the partial pressure of water to the saturation (vapor) pressure of water at a specified temperature].[29] Moreover, a good

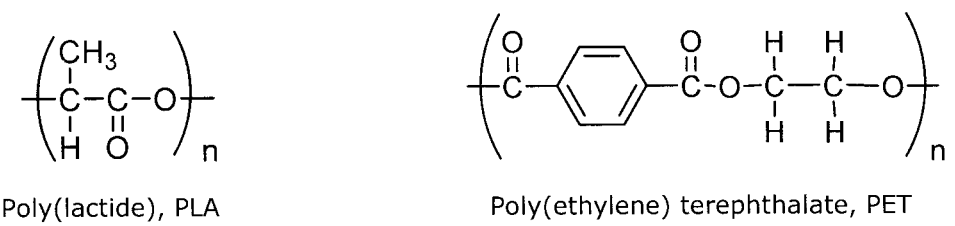

Scheme 2 Constituent units of PLA and PET.

approximation of the moisture content in the range of 0–0.1A_w is given by 0.000125 × A_w. For PLA pellets, Witzke[16] reported an absorption of less than 8000 ppm (w/w) at A_w = 0.9. Therefore, in polymers such as PET and PLA, that absorb very low amounts of water, the effect of water can also be crucial to the polymer barrier properties and general performance. For example, in the case of PET, water plasticizes the amorphous phase, which leads to a decrease in T_g from about 80°C in a dry state to about 57°C in a saturated state and a consequent reduction of the elastic modulus.[28] For PLA, a significant change in T_g as a function of the water content was has also been reported.[30] Besides the changes in the physical and mechanical properties, surprising changes in the polymer barrier properties and diffusion mechanism can happen as a result of the presence of relatively small quantities of absorbed water. For PET, early studies have shown that the diffusion coefficient follows Fick's first law[31] and that oxygen solubility follows Henry's law.[32] Also, recent studies performed on the oxygen barrier properties of amorphous copolyesters based on ethylene terephthalate with different crystallinities have shown that PET films obey Fick's first law at A_w = 0.[33,34] Because the presence of water has a significant effect on the mechanical and barrier properties, PET and PLA polymers may show variations of the oxygen permeability coefficient as the water content increases.

The aim of this work was to study the variations of the oxygen diffusion, solubility, and permeability coefficients of PET and PLA films at different temperatures (5, 23, and 40°C) and A_w values (0–0.9). The water sorption isotherm for PLA films was determined. The T_g, T_m, and crystallinity values of PLA and PET polymers were also measured.

EXPERIMENTAL

Materials

Two PLA films, identified as 4031-D and 4041-D, were provided by Cargill-Dow LLC Polymers (Blair, NB). 4031-D was nominally made with 98% L-lactide, and 4041-D was nominally made with 94% L-lactide; the densities were 1240 and 1243 kg/m^3, respectively. PLA 4041-D had a low molecular weight PLA sealant layer on the inside part of the film. A standard commercial PET film was used to measure the PET barrier properties. The films were studied as received.

Methods

Thickness

The thickness of the films was determined with a TMI 549M micrometer (Testing Machines, Inc., Amityville, NY) according to ASTM D 374-99.

Thermal characterization

A differential scanning calorimeter (DSC 2010) from TA Instruments (New Castle, DE) was used to determine T_g and T_m (ASTM D 3418-97) and the enthalpy of fusion for PLA and PET polymers (ASTM D 3417-97). The crystallinity of the polymers was calculated from the enthalpies.

Water sorption isotherm

Saturated salt solutions of lithium chloride (LiCl), magnesium chloride ($MgCl_2$), magnesium nitrate [$Mg(NO_3)_2 2H_2O$], sodium chloride (NaCl), potassium chloride (KCl), and potassium nitrate (KNO_3) were used to provide A_w's of 0.11, 0.33, 0.52, 0.75, 0.85, and 0.94, respectively. All chemicals were analytical-grade and were obtained from EM Science (Gibbstown, NJ). The aforementioned saturated solutions were put into different desiccators, to which the samples were added. The sorption experiments were carried out with film specimens (0.5 cm × 3 cm) conditioned at A_w = 0.5 at 23°C before they were exposed to different A_w's at 5, 23, and 40°C. The initial moisture content of the PLA films (in triplicate) was measured on a dry-weight basis via drying in a hot-air vacuum oven at 60°C for 10 h. The samples were weighed until equilibrium (±0.0001 g), and a Metrohm Karl Fischer Titrator K 720 from Metrohm, Ltd. (Herisau, Switzerland) was used to determine the final moisture content.

Oxygen permeability

A modified Oxtran 100-Twin with a coulometric sensor (Mocon, Inc., Minneapolis, MN) was used for measuring the permeability of oxygen through the polymer films as a function of A_w. The experiments were carried out at 0.21 atm of pressure for PLA films and at 1 atm of pressure for PET films. Figure 1 shows a schematic diagram of the test apparatus, which was similar to one used by previous researchers.[27] Before a polymer film was mounted in a cell, each film was vacuum-dried at 60°C for at least 10 h. After the films were mounted to cells A and B (Fig. 1), a stream of dry nitrogen was circulated through the system. For each A_w value at which the permeability of oxygen was measured, a nitrogen stream adjusted to the selected A_w value flowed throughout a cell containing a film for at least 24 h.

During this period, each film acquired a moisture content in equilibrium with that in the nitrogen stream. The initial time was marked when an oxygen gas stream at the selected A_w value, equal to A_w of the film in the cell, was introduced. The amount of oxygen that permeated per unit of time was continuously monitored with a Mocon D-200 integrator until a

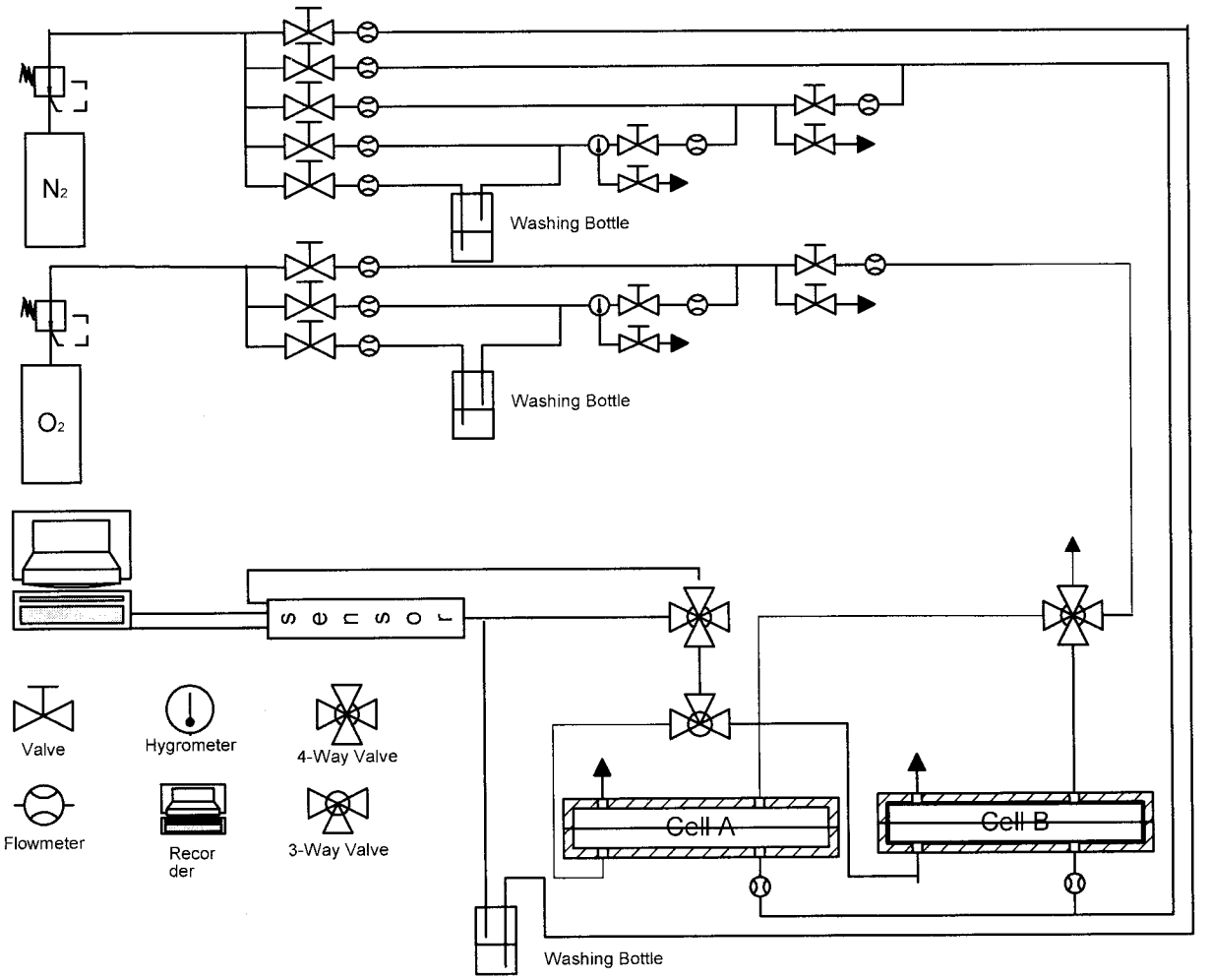

Figure 1 Schematic diagram of the test apparatus for permeability experiments.

steady state was reached (i.e., the oxygen flux changed by less than 1% for 30 min). The instrument was calibrated at each temperature at which the samples were tested (i.e., 5, 23, and 40°C) through the measurement of the oxygen flow rate through a standard reference material provided by Mocon. A_w values were determined with a Hygrodynamics model 1820A wide-range humidity sensor from Newport Scientific, Inc. (Jessup, MD).

The experimental error in the determination of the oxygen flow rate on the Oxtran 100-Twin apparatus was estimated to be 2–5%, with highly reproducible and consistent readings. The experimental error in the measurement of A_w was estimated to be 2%.

Theoretical background

The data obtained were analyzed with a consistency test for isostatic permeability experiments.[35] This test permits the detection of any significant variations of temperature and concentration during an experiment, and it also provides information about the diffusion and sorption mechanism of the oxygen in the polymer. In the isostatic method used in this research, nitrogen/2% H_2 (carrier gas) is routed through the lower half of the cell. Oxygen or compressed air (test gas) is fed through the upper test cell. Oxygen permeates through the specimen and is picked up by the carrier gas. The amount of oxygen in the carrier gas detected by the coulometric sensor is proportional to the amount of oxygen that permeates the polymer. At the beginning of the permeation process (i.e., the transient state), the oxygen concentration is changing with time. After that, the permeation process reaches a steady state at which the oxygen concentration is independent of time. The amount of oxygen (F) that permeates a thin sheet can be obtained from the general diffusion equation:

$$F = -D\nabla c \tag{1}$$

When the diffusion coefficient (D) is independent of the concentration (c), the one-dimensional solution of eq. (1) can be expressed as eq. (2), which describes the

process mentioned previously with boundary conditions according to Fick's second law[36] for a film sheet tested by an isostatic permeation experiment:[35]

$$\frac{F_t}{F_\infty} = \left(\frac{4}{\sqrt{\pi}}\right)\left(\sqrt{\frac{l^2}{4Dt}}\right) \sum_{n=1,3,5...}^{\infty} \exp\left(\frac{-n^2l^2}{4Dt}\right) \quad (2)$$

where F_t is the flow rate of oxygen permeating the film at the transient state at time t, F_∞ is the oxygen transmission rate at the steady state, l is the film thickness, and D is the oxygen diffusion coefficient. For the application of the consistency test, eq. (2) is simplified to eq. (3), which describes the permeation for a flow ratio of 0.05–0.95:[35]

$$\phi = \frac{F_t}{F_\infty} = \left(\frac{4}{\sqrt{\pi}}\right) X^{1/2} \exp(-X) \quad (3)$$

where X is equal to $l^2/4Dt$ and ϕ is the ratio between the flow rates at time t and in the steady state. From the isostatic method, ϕ is obtained from time zero to the time at which the polymer reaches the steady state. Therefore, with a Newton–Raphson method,[37] the value of X can be calculated for each value of t, and D can be obtained from the slope of $1/X$ versus time. The plot of $1/X$ as a function of time is expected to be a straight line, which intercepts the origins of both axes. By this method, it is also possible to determine two constants (i.e., K_1 and K_2), which are the ratios of the X values at $\phi = 0.50$ and $\phi = 0.75$ divided by the value of X at $\phi = 0.25$. If an error level of 5% is considered acceptable, the values obtained for these two constants are as follows: $0.42 \leq K_1 \leq 0.46$ and $0.65 \leq K_2 \leq 0.69$.[35,38] The calculation of K_1 and K_2 permits the evaluation of whether isostatic tests have been carried out under the right conditions and also checks the diffusion mechanics that take place. In addition, from the transient flow rate profile, the half-time diffusion coefficient (D) can be estimated as follows:[36]

$$D = \frac{l^2}{7.199t_{0.5}} \quad (4)$$

After that, a procedure based on the sum-of-squares technique is applied to determine the best estimated diffusion coefficient value from eq. (2).[39] Next, the diffusion coefficients obtained for the continuous-flow method and by the sum of squares are compared. The steady-state time is calculated by the solution of eq. (2) when ϕ is equal to one, with the diffusion coefficient obtained from the previous step. With the value of the permeant flow in the steady state (F_∞), the permeability coefficient (P) can be determined as follows:

$$P = \frac{F_\infty l}{A\Delta p} \quad (5)$$

where A is the area of the film and Δp is the partial pressure gradient across the polymer film. Then, if Henry's law of solubility is applied to oxygen diffusion in films at low pressures (i.e., up to 1 atm), the solubility coefficient (S) can be calculated as follows:

$$P = SD \quad (6)$$

The temperature dependence of P, S, and D can be described by Van't Hoff–Arrhenius equations:[40]

$$S(T) = S_0 \exp(-\Delta H_S/RT) \quad (7)$$

$$D(T) = D_0 \exp(-E_D/RT) \quad (8)$$

$$P(T) = P_0 \exp(-E_P/RT) \quad (9)$$

where ΔH_S is the molar heat of sorption, E_D is the activation energy of diffusion, and E_P is the apparent activation energy of permeation. It is easy to see that

$$P_0 = S_0 D_0 \quad (10)$$

$$E_P = \Delta H_S + E_D \quad (11)$$

ΔH_S can be expressed as the sum of the heat of condensation (ΔH_C) and the heat of mixing (ΔH_M):

$$\Delta H_S = \Delta H_C + \Delta H_M \quad (12)$$

P_0, S_0, D_0, E_P, ΔH_S, and E_D can be derived from isostatic permeation experiments.

Finally, as a first approximation and because oxygen is insoluble in the crystalline part of PET films,[31,32] the diffusion, solubility, and permeation coefficients for semicrystalline polymers can be estimated as follows:

$$D_{sc} = D_a(1 - \chi_c) \quad (13)$$

$$S_{sc} \approx S_a(1 - \chi_c) \quad (14)$$

$$P = D_{sc}S_{sc} = D_aS_a(1 - \chi_c)^2 \quad (15)$$

where χ_c is the degree of crystallinity and D_a and S_a are the diffusion and solubility coefficients, respectively, in the amorphous part of the polymer.

RESULTS AND DISCUSSION

Thickness

Because the main source of error in calculating D [eq. (4)] and P [eq. (5)] was the thickness, special care was taken to determine the film thickness. The thickness of PLA and PET films was determined according to ASTM D 374-99. For 4031, it was 23.2 μm (0.913 mil),

TABLE I
DSC Results for PLA and PET

	4031-D	4041-D	PET
T_g (°C)	71.4	66.1	80
Relaxation enthalpy (J/g)	1.4	2.9	N/A
T_m (°C)	163.4	140.8	245
Enthalpy of fusion (J/g)	37.5	21.9	47.7
Crystallinity percentage	40	25	38

N/A = not applicable.

and for 4041, it was 28.5 μm (1.1 mil). For PET, the thickness was 23.4 μm (0.921 mil).

Thermal characterization

PLA films undergo an endothermic event that is superimposed on T_g and observed during the first differential scanning calorimetry (DSC) heating.[17] This endothermic relaxation is indicated in Table I. Also, Table I presents T_g and T_m and the enthalpy of fusion for both PLA and PET films. The crystallinity percentage (χ_c) can be evaluated as follows:

$$\chi_c = 100 \frac{\Delta H_m}{\Delta H_m^c} \tag{16}$$

where ΔH_m is the enthalpy of fusion and ΔH_m^c is the heat of melting of purely crystalline poly(L-lactide) or PET. For PLA, ΔH_m^c is 93 J/g,[41] and for PET, ΔH_m^c is 125.6 J/g.[42] PLA 4031-D and 4041-D show lower T_g and T_m values than PET films.

Water sorption isotherm

PLA films stored for more than 1 week at 5, 23, or 40°C and at A_w = 0.11, 0.33, 0.52, 0.75, 0.85, or 0.94 were periodically weighed with a precision of ±0.0001 g and dried in a vacuum oven. Because the average samples were approximately 0.2 g, a minimum water absorption value of 500 ppm could be detected with this technique. Metrohm Karl Fischer Titrators K 720 equipment can measure water absorption with a sensitivity of 100 ppm. Neither technique was able to measure water absorbed in PLA at any value of A_w.

Having 33% acyl ester bonds in its backbone, PLA is more susceptible to hydrolysis than many commercial types of polyester. Previous studies of amorphous PLA pellets (number-average molecular weight = 50,000–100,000 Da) with a porosity of 8.24%, a total pore area of 36.8 m^2/g, and an average pore diameter of 0.0072 μm indicated low amounts of water absorption (i.e., 8000 ppm at 25°C and A_w = 0.9, with an equilibrium time no higher than 72 h).[16] Also, the same researchers have reported that water absorption is fairly insensitive to moderate temperature changes. PLA is moderately polar, with a solubility parameter (δ) of 19–20.5 $MPa^{0.5}$.[4] δ of water is 48 $MPa^{0.5}$. When the difference between the δ values of the water and polymer is higher, the water sorption decreases. For PET, δ is 16 $MPa,^{0.5}$ and the water absorption is 60 ppm at 25°C at A_w = 0.5. For polystyrene (PS) (δ = 19 $MPa^{0.5}$), the water absorption is 320 ppm at 25°C at A_w = 0.5.[16] Therefore, in the case of PLA, an amount of water absorbed between the amounts absorbed for PET and PS films was expected. However, we were not able to measure water absorption in either of the PLA films studied. Some of the difference between the amounts of water absorbed by the pellets and the films could be explained by the differences in crystallinity; in addition, some of the water measured in the pellets could be trapped in the porous structure, rather than absorbed in PLA. Because a low water content at equilibrium is expected for PLA films, further research with more sensitive instrumentation is needed.

Oxygen permeability

The diffusion, solubility, and permeability coefficients of PET and PLA were determined by the isostatic technique at 1 and 0.21 atm of pressure, three temperatures (5, 23, and 40°C), and A_w values of 0, 0.3, 0.6, and 0.9. Four different A_w values were selected because PET and PLA films do not absorb much water and also do not show much variation of water absorbed as the temperature increases.[17,30]

PET

Representative plots of oxygen permeation as a function of time are presented in Figure 2 for PET films at 5, 23, and 40°C at A_w = 0.9 and in Figure 3 for PET films at 40°C and A_w = 0, 0.3, 0.6, and 0.9.

Figures 2 and 3 show a faster transient state as A_w and the temperature increased. Figure 3 also shows that not much variation of the oxygen flow fraction was found at $A_w < 0.3$. The behaviors shown in Figures 2 and 3 were found at the three different temperatures at which the polymer films were tested. In both figures, a good correlation between the experimental values and the values calculated by eq. (1) can be observed.

The permeability coefficients at different A_w values and temperatures were calculated with eq. (4) (see Fig. 4).

Figure 4 shows that the values of the oxygen permeability coefficients decreased as the temperature decreased. The oxygen permeability coefficient tended to decrease as A_w in the oxygen stream increased; this is the opposite of the effect shown by hydrophilic polymers.[26] This decrease in the oxygen permeability coefficient was more significant at 40°C than at 23 and 5°C. The values of the permeability coefficients ob-

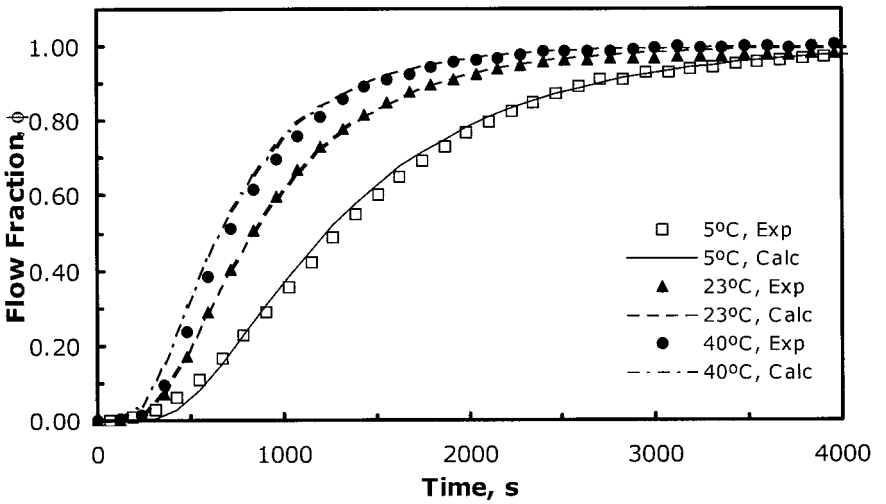

Figure 2 Permeant flow fraction versus time for oxygen permeation experiments for PET films at 5, 23, and 40°C ($A_w = 0.6$).

tained in this research are similar to the values found in the literature;[34] however, they are a little lower (e.g., the oxygen permeability coefficient of PET reported in the literature was 7.64×10^{-19} kg m/m^2 s Pa at 25°C and at $A_w = 0$[34]). This can be explained by the differences in the crystallinity and the final polymer treatment.

The values of the oxygen diffusion coefficient versus A_w obtained from the unsteady state by the consistency test for isostatic permeability experiments are shown in Figure 5. An exponential increase in the diffusion coefficient as A_w increases can be observed, and an increase in the oxygen diffusion coefficient as temperature increases is also evidenced. This effect is also more pronounced at 40°C than at 23 and 5°C. The increase in the oxygen diffusion coefficient at higher A_w values can be attributed to a major plasticization effect of the amorphous PET phase by the water molecules. The plasticization effect, as in hydrophilic polymers, tends to increase the mobility of the oxygen molecules in the polymer bulk phase. This plasticization effect is evidenced by the reduction of T_g. For PET, water plasticization leads to a decrease in T_g from about 80°C in a dry state to about 57°C in a saturated state.[28] Although PET shows a reduction of T_g, the clustering of water molecules has not been reported.[43] Thus, if we compare the values of the diffusion coefficients obtained in this research at 25°C, they are one order of magnitude lower than the values found in the literature[34] (i.e., the oxygen diffusion coefficient of PET was reported to be 5.6×10^{-13} m^2/s at 25°C at $A_w = 0$ and 11.6×10^{-13} m^2/s at 40°C at $A_w = 0$[34]). This can be explained by the different crystallinity and processing conditions of the films used.

Figure 6 presents the values of the solubility coefficient versus A_w for PET films at 5, 23, and 40°C. An

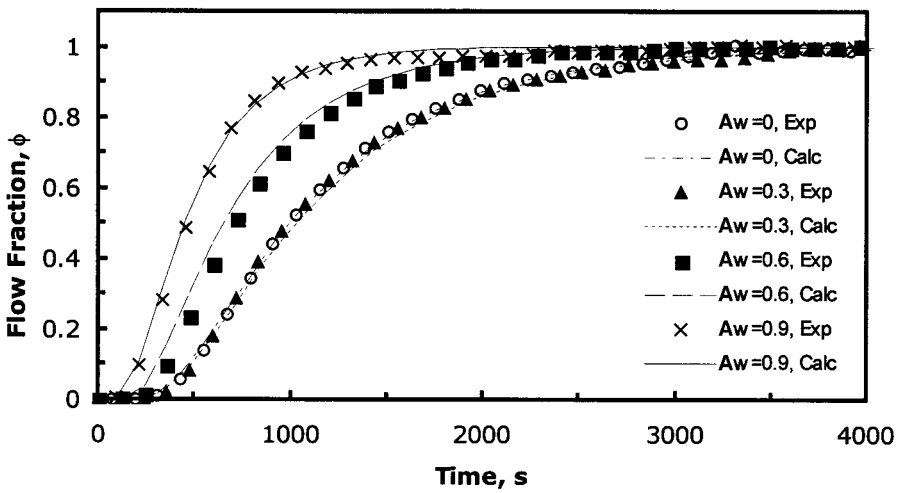

Figure 3 Permeant flow fraction versus time for oxygen permeation experiments for PET films at 40°C ($A_w = 0$, 0.3, 0.6, or 0.9).

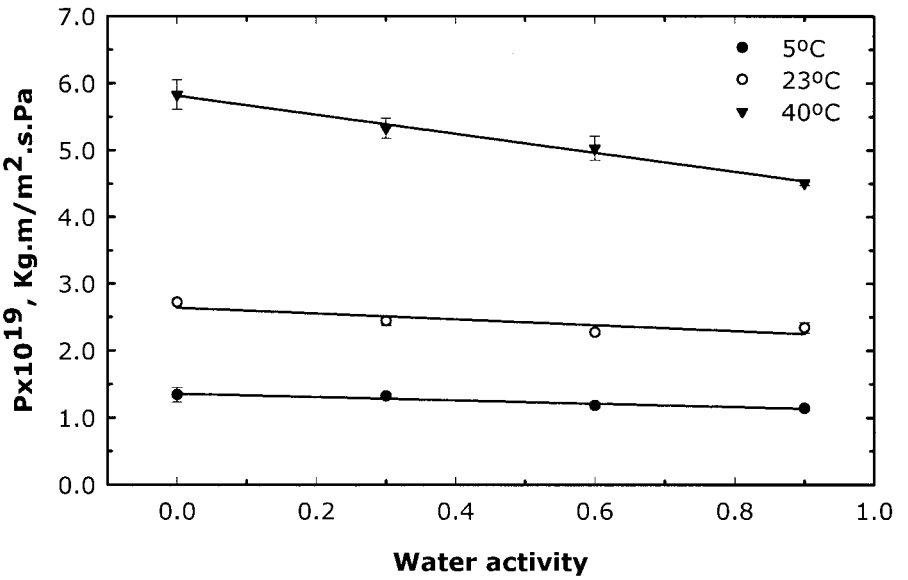

Figure 4 PET oxygen permeability coefficient (P) versus A_w at 5, 23, and 40°C.

increase in the solubility coefficient as the temperature increased was observed, and a reduction of the solubility coefficient as A_w increased was evident. Henry's law is obeyed for PET films in the range of 0–1.0 atm.[32] However, the contribution of Henry's law mechanism is small in PET films. Instead, sorption is the process of filling the holes of free volume, and the solubility should be proportional to the amount of free volume.[33,34,44] Because PET solubility is directly proportional to the free volume of the amorphous polymer matrix,[31] a reduction of the free volume available will produce a decrease in the solubility. Therefore, the linear variation of the solubility coefficient as A_w increased can be explained by a competition between the water and oxygen molecules for the free volume. When A_w increased and, therefore, the amount of water sorbed into the polymer also increased, the solubility of oxygen decreased. Because the permeation of water in PET polymers is faster than the oxygen permeation (i.e., the water permeability is $P = 1.1 \pm 0.1 \times 10^{-15}$ kg m/m^2 s Pa at 25°C between $A_w = 0.4$ and $A_w = 0.9$[17]), the free volume is filled first with water molecules and then with oxygen. Therefore, the net effect of the presence of water would be an increase in

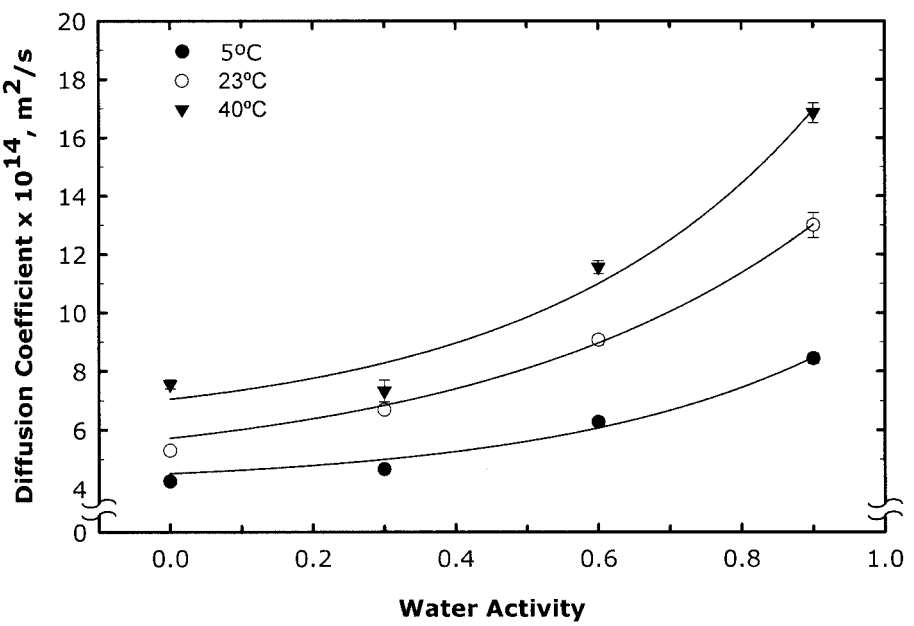

Figure 5 Diffusion coefficient of PET films as a function of A_w.

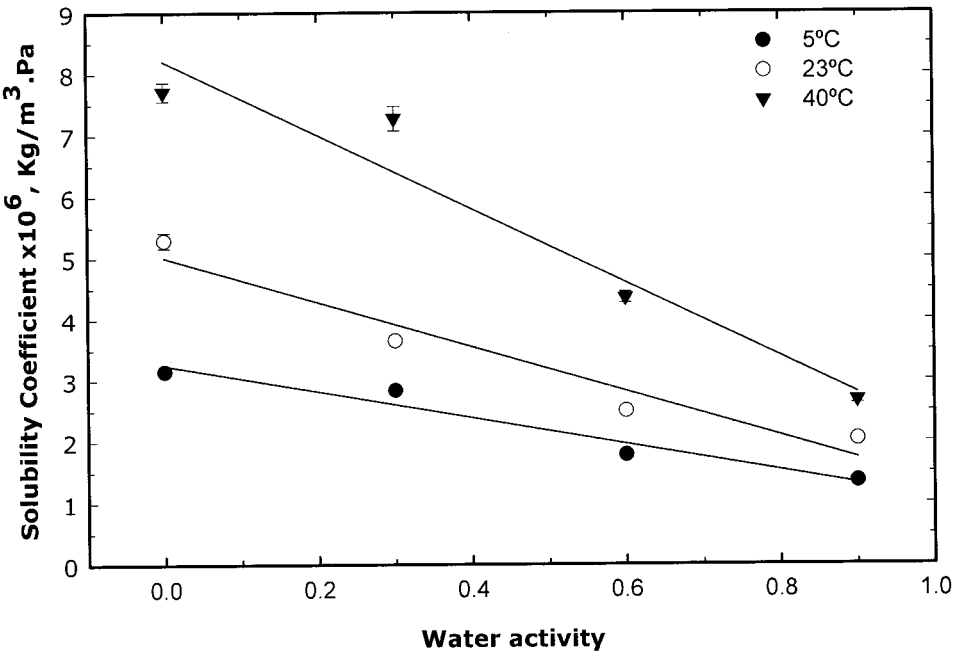

Figure 6 Solubility coefficient of PET films as a function of A_w.

the diffusion coefficient and a reduction of the solubility coefficient. Similar behavior was observed in PET films with the mutual permeation of nitrogen and oxygen.[45] Because the oxygen diffused more quickly than the nitrogen, the solubility of nitrogen decreased and the diffusion of nitrogen increased as the oxygen concentration increased. The values of the solubility coefficient obtained in this research are higher than the values found in the literature (i.e., the oxygen solubility coefficient of PET is reported in the literature to be 1.38×10^{-6} kg/m^3 Pa at 25°C at $A_w = 0$[34]).

PLA 4031 and 4041

Figures 7 and 8 represent the oxygen permeability coefficient for PLA polymers as a function of A_w. A significant increase in the oxygen permeability coefficient as the temperature increased can be observed for 4031 and 4041. PLA 4031 showed an increase in the oxygen permeability coefficient from 3.5×10^{-18} kg m/m^2 s Pa at 5°C to 11×10^{-18} kg m/m^2 s Pa at 40°C when moisture was not present. Under higher A_w levels ($A_w = 0.9$), the value of the oxygen permeability coefficient increased only to 8.5×10^{-18} kg m/m^2 s Pa at 40°C. This reduction of the oxygen permeability coefficient as A_w increased at a constant temperature can be observed in Figure 7 for the three temperatures tested. The reduction of values was more pronounced at 40°C. The same behavior presented in 4031 can be observed in Figure 8 for 4041. However, the values of the oxygen permeability coefficient for 4041 were approximately 10% lower at each temperature. A higher variation of the oxygen permeability coefficient at 23 and 40°C can be observed for 4041 than for 4031.

The difference between the values of oxygen permeability measured in this research and the values measured in previous studies[6] of 3.53×10^{-17} kg m/m^2 s Pa at 30°C and $A_w = 0$ for PLA biaxially oriented films can be explained by the differences in the crystallinity and final processing conditions of both films.

The oxygen diffusion coefficients of 4031 and 4041 are represented in Figures 9 and 10. Behavior similar to that shown for PET films in Figure 5 can be observed for both PLA films. As for PET films, the oxygen diffusion coefficient increased as the temperature increased. Also, an exponential increase of the oxygen diffusion coefficients from 2×10^{-14} to 9×10^{-14} m^2/s at 23°C can be observed as A_w increased from 0 to 0.9. The observed increase of the oxygen diffusion coefficient in the range of $A_w = 0$–0.9 can also be attributed to the plasticization effect on the amorphous phase by the water molecules. As in PET, plasticization effects tend to increase the mobility of the oxygen molecules in the polymer matrix. Plasticization effects are evidenced by a reduction of the polymer T_g. In previous work,[30] it was shown that the variation of T_g was significant when the samples were stored for 7 days at 5, 23, or 40°C and at different relative humidities. Some authors attribute this reduction of T_g in hydrophilic films to the clustering of water in the polymer matrix.[26] However, in the case of PLA and other hydrophobic films, clusters of water have not been reported in the polymer matrix.[16,33,34] PLA 4031 has a

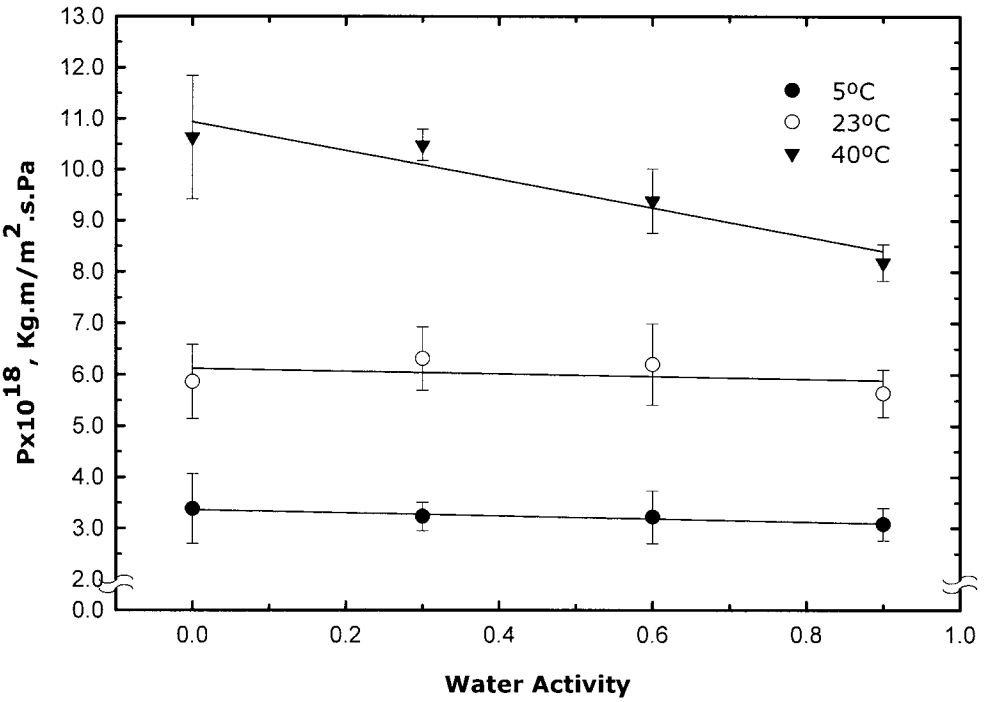

Figure 7 Oxygen permeability coefficient (P) as a function of A_w for PLA 4031.

higher crystallinity than 4041,[17] which generates a more tortuous path for the permeation of oxygen molecules. As a result, the oxygen diffusion coefficient of 4041 is generally higher than that of 4031 at different temperatures and relative humidities. 4041 has a lower molecular weight inner sealant layer that enhances the diffusion of oxygen. The values of the diffusion coefficient for 4041 are not as consistent as those for 4031. One of the reasons for this inconsistency could be the sealant layer present in 4041.

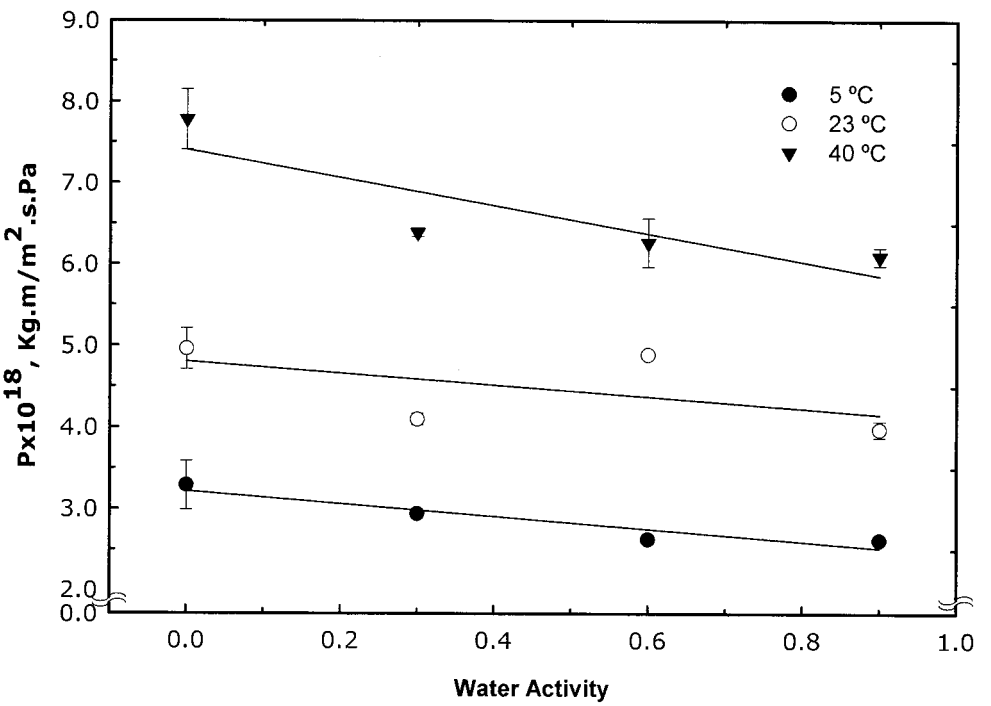

Figure 8 Oxygen permeability coefficient (P) as a function of A_w for PLA 4041.

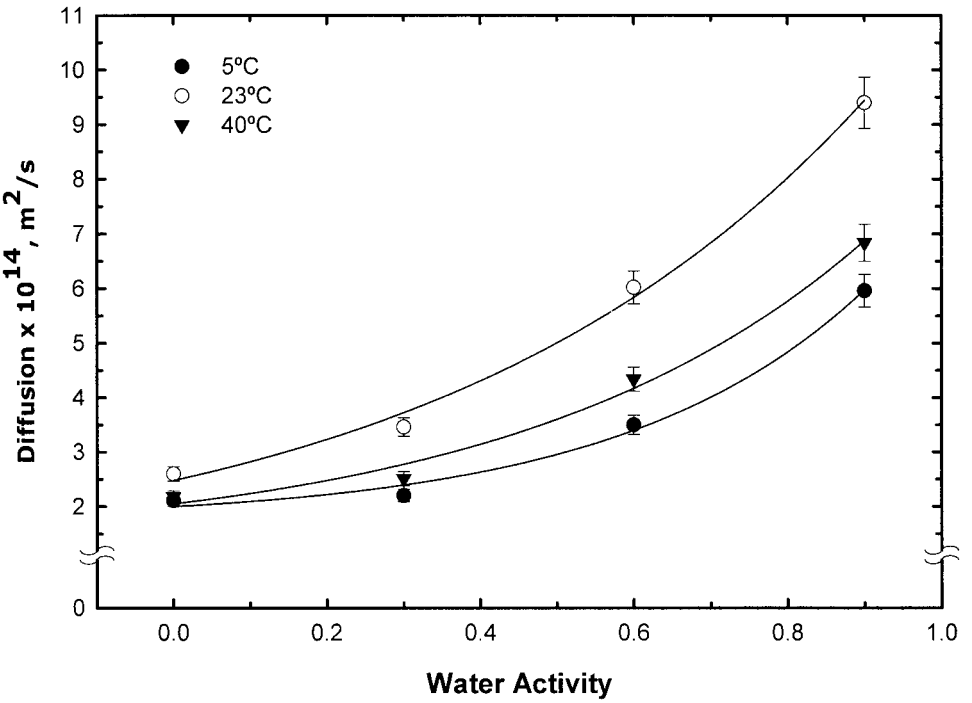

Figure 9 Oxygen diffusion coefficient of 4031 films as a function of A_w.

Figures 11 and 12 present the values of the oxygen solubility coefficient in PLA films. Figure 11 shows the variation of the solubility coefficient for 4031. The oxygen solubility coefficient increased as the temperature increased. A linear reduction of the solubility coefficient from 5 to 1.5 $\times$ 10^{-4} kg/m^3 Pa at 40°C can be observed as A_w increased from 0 to 0.9. This reduction can be explained, as for PET, by the occupancy of the free volume by water molecules at higher water contents; therefore, a reduction of the oxygen solubility as the water content increased can be observed. In the case of 4041, Figure 12 shows a more erratic behavior of the solubility coefficient across the A_w values. However, as in 4031, the tendency of a lower

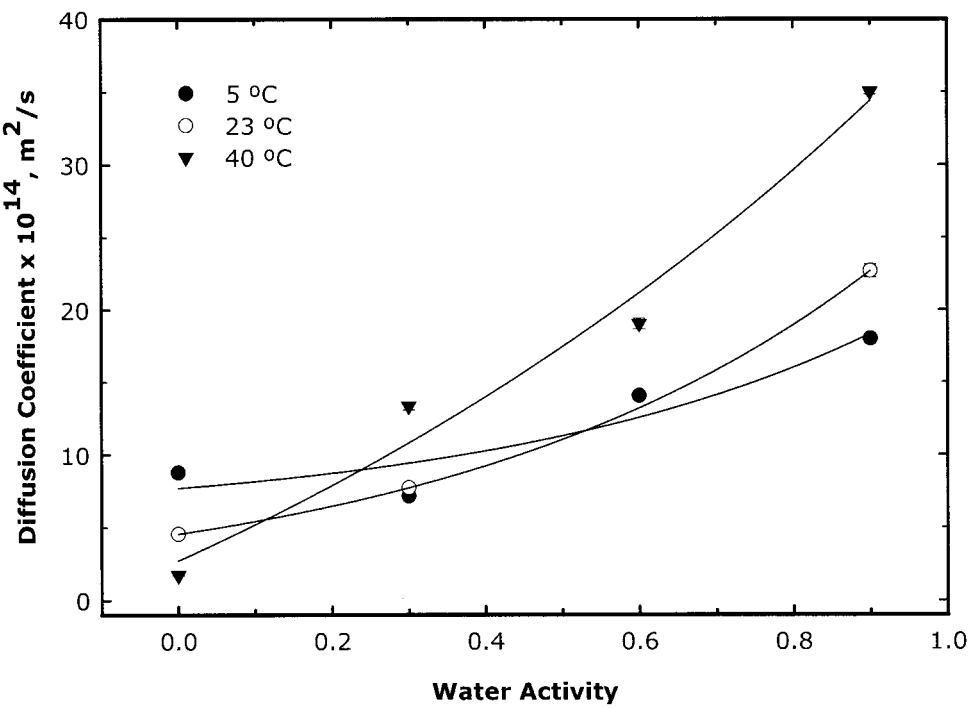

Figure 10 Oxygen diffusion coefficient of 4041 films as a function of A_w.

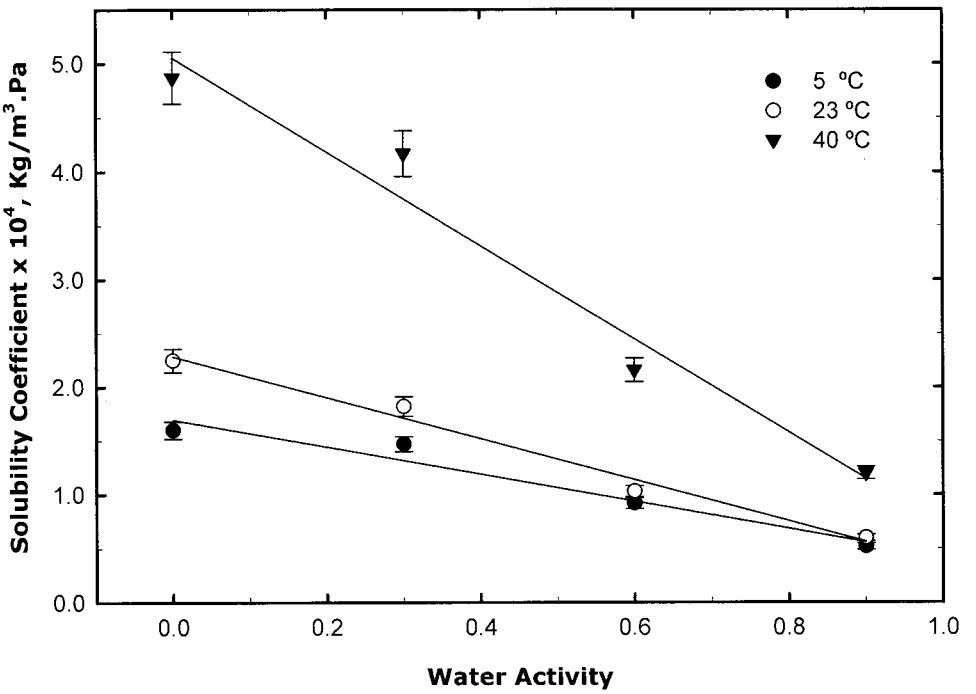

Figure 11 Solubility coefficient of PLA 4031 films as a function of A_w.

solubility coefficient as A_w increases is significant. In addition, a significant increase of the solubility coefficient as the temperature increased is evidenced. The nonuniform nature of the solubility coefficient for 4041 may also be attributed to the inner sealant layer.

ΔH_S was calculated with the Van't Hoff's equation as a function of A_w [eq. (7)]. E_D was estimated with the Arrhenius equation [eq. (8)]. Finally, the values of E_P were calculated with eq. (9). In addition, the values of P_0, S_0, and D_0 were estimated with eqs. (7)–(9). The results are presented in Table II. The values of ΔH_S and its pre-exponential factor for 4041 were not calculated because of the higher variability in the determination.

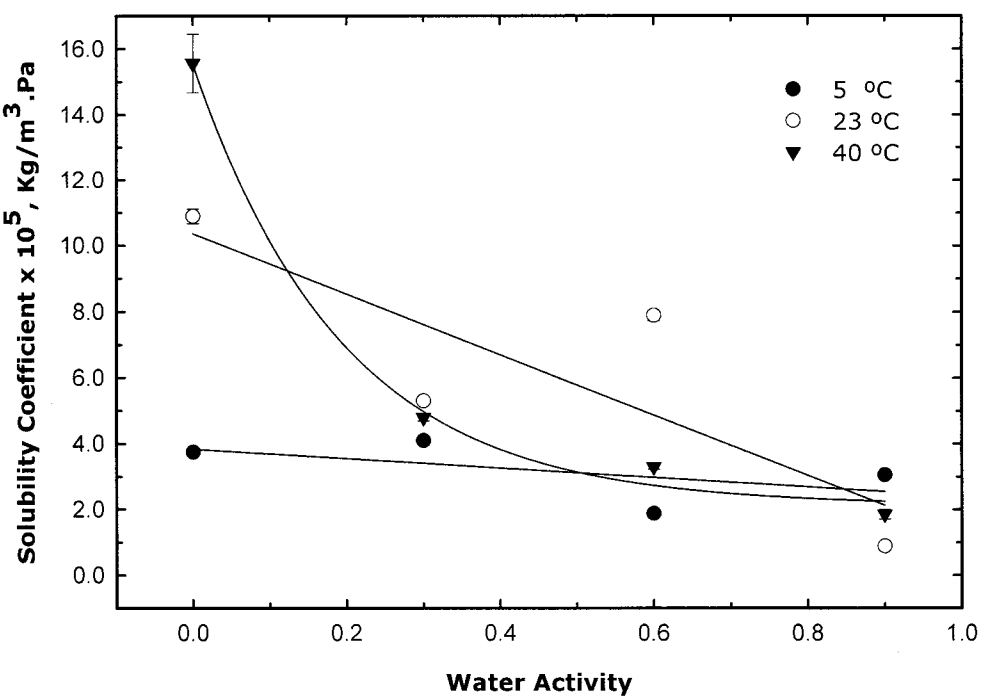

Figure 12 Solubility coefficient of PLA 4041 films as a function of A_w.

TABLE II
Preexponential Terms of Eqs. (7–9) and ΔH_S, E_P, and E_D in Oxygen Mass Transport Through PET and PLA Films at different A_W Levels

Material	A_W	$P_0 \times 10^{14}$ (kg m/m^2 s Pa)	E_P (kJ/mol)	$D_0 \times 10^{12}$ (m^2/s)	E_D (kJ/mol)	$S_0 \times 10^3$ (kg/m^3 Pa)	ΔH_S (kJ/mol)
PET	0.0	6.24	30.30	6.63	11.76	9.68	18.54
	0.3	2.99	28.60	2.9	9.47	10.2	19.13
	0.6	4.75	29.93	10.1	11.62	4.69	18.31
	0.9	2.41	28.36	38.9	14.22	0.62	14.14
4031	0.0	9.00	23.62	300.00	0.96	2667.80	22.65
	0.3	12.4	24.38	981.00	3.18	1264.44	21.19
	0.6	4.86	22.18	34.20	4.97	141.901	17.21
	0.9	2.00	20.24	27.84	3.29	72.04	16.94
4041	0.0	3.01	21.12	0.0004	12.07	N/A	N/A
	0.3	0.90	18.67	14.90	12.51	N/A	N/A
	0.6	3.07	21.60	0.93	5.05	N/A	N/A
	0.9	1.99	20.63	17,202.28	28.04	N/A	N/A

N/A = not applicable.

The average E_P value for PET was 29.3 ± 0.96 kJ/mol, and P_0 was 4.09 ± 1.74 kg m/m^2 s Pa. E_D increased from 11.76 kJ/mol at $A_w = 0$ to 14.22 kJ/mol at $A_w = 0.9$. An increase in the values of the oxygen diffusion activation energy indicates that the diffusing molecule must overcome larger intermolecular forces within the polymer at higher water contents to diffuse. Together with the increase of E_D, a reduction of ΔH_S was observed at higher humidity contents. If we compare the values of the activation energy of permeation with the value reported in the literature[46] (E_P = 32 kJ/mol at $A_w = 0$), a good agreement can be seen. The values of E_D reported in this research are lower than the values reported in the literature.

E_P for PLA 4031 (23.39 ± 1.11 kJ/mol) is mainly constant between $A_w = 0$ and $A_w = 0.6$. However, a reduction of the activation energy at $A_w = 0.9$ of almost 2 kJ/mol is evidenced. E_D increases from 0.96 kJ/mol at $A_w = 0$ to 3.29 kJ/mol at $A_w = 0.9$, with the major increase between $A_w = 0$ and $A_w = 0.3$. If we compare the values of the activation energy of PLA 4031 and PET, we can see that PLA presents less resistance to oxygen diffusion than PET. Also, the increase of E_D is accompanied by a reduction in ΔH_S for PLA 4031 from 22.65 kJ/mol at $A_w = 0$ to 16.94 kJ/mol at $A_w = 0.9$.

4041 presents a smaller reduction of the activation energy at higher humidity levels. The difference between the oxygen permeation activation energy measured in this research and that reported in previous research[6] (E_P = 11.2 kJ/mol at $A_w = 0$) may be explained by the difference in the polymer crystallinity and processing conditions.

For condensable vapors such as water, ΔH_C is negative (−42 kJ/mol). For oxygen, ΔH_C is negative and equal to −7.5 kJ/mol. ΔH_M is positive for hydrophobic polymers and near-zero or negative for polar polymers.[47] Table III indicates the values of ΔH_M calculated by eq. (11) for PET and PLA 4031 films.

For PET, according to eq. (12), ΔH_M is equal to 25.03 ± 1.11 kJ/mol between $A_w = 0.3$ and $A_w = 0.6$ and 21.7 kJ/mol at $A_w = 0.9$.

Early studies[31,32] of PET films showed that oxygen only dissolves in the amorphous part of the polymer films. Because the crystallization of polymers tends to reduce the volume of amorphous material available for diffusion, the diffusion coefficient and the solubility of the amorphous polymers are higher than those of glassy crystalline polymers. D_a, and S_a for PET and PLA can be calculated from eqs. (13) and (14). For PET, χ_c is 38 at 23°C and $A_w = 0$, D_a is 8.31 × 10^{-14} m^2/s, and S_a is 8.53 × 10^{-6} kg/m^3 Pa; for PLA 4031-D at 23°C and $A_w = 0$, χ_c is 0.40, D_a is 4.33 × 10^{-14} m^2/s, and S_a is 3.76 × 10^{-4} kg/m^3 Pa.

The values of D_a and S_a obtained for amorphous PET from the literature at $A_w = 0$ are $D_a = 5.6 \times 10^{-13}$ m^2/s at 23°C[33] and $S_a = 1.38 \times 10^{-6}$ kg/m^3 Pa at 23°C.[33] The diffusion coefficient values obtained in this research are lower than those previously reported, and the solubility values are higher. For PLA, no comparison values were found in the literature.

Previous research[30] showed that for 4031-D, no statistically significant changes in the enthalpy of fusion and crystallinity as functions of time, temperature, and humidity could be found ($P > 0.05$). Table IV gives the results for the diffusion and solubility coefficients of amorphous PLA 4031 at different water contents. 4041-D

TABLE III
ΔH_M Calculated by Eq. (11) for PET and 4031

A_W	ΔH_M (kJ/mol)	
	PET	PLA 4031
0	26.04	30.15
0.3	26.63	28.69
0.6	25.81	24.79
0.9	21.64	24.44

TABLE IV
D_a and S_a for PLA 4031

	PLA 4031 (χ_c = 0.40)	
A_W	$D_a \times 10^{14}$ (m^2/s)	$S_a \times 10^4$ (kg/m^3 Pa)
0	4.33	3.76
0.3	5.77	3.04
0.6	10.40	1.71
0.9	15.66	1.00

shows a statistically significant change in the enthalpy of fusion as a function of time ($P < 0.05$). A reduction of 30% of the enthalpy of fusion from the initial day was recorded, which can explain the different behaviors of the solubility coefficients.

In conclusion, PET and PLA are both hydrophobic films that absorb very low amounts of water, and they show similar barrier property behaviors, as shown in this research.

CONCLUSIONS

The oxygen barrier properties of PET and PLA films at three different temperatures (5, 23, and 40°C) were measured. The permeability coefficients of PET and PLA decreased as the water content increased. An increase in the permeability coefficient of PET and PLA was observed as the temperature increased. Oxygen diffusion in PET and PLA showed an exponential increase as A_w increased at each temperature. The effect was more pronounced at higher temperatures. The oxygen solubility coefficient decreased linearly as A_w increased because of the reduction in the free volume due to its occupation by water molecules.

The authors thank Cargill Dow LLC for the polymer samples.

References

1. Mainil-Varlet, P.; Curtis, R.; Gogolewski, S. J Biomed Mater Res 1997, 36, 360.
2. Ikada, Y.; Tsuji, H. Macromol Rapid Commun 2000, 21, 117.
3. Bleach, N. C.; Tanner, K. E.; Kellomaki, M.; Tormala, P. J Mater Sci: Mater Med 2001, 12, 911.
4. Tsuji, H.; Sumida, K. J Appl Polym Sci 2001, 79, 1582.
5. Dorgan, J. R.; Lehermeier, H. J.; Palade, L.-I.; Cicero, J. Macromol Symp 2001, 175, 55.
6. Lehermeier, H. J.; Dorgan, J. R.; Way, D. J Membr Sci 2001, 190, 243.
7. Benicewicz, B. C.; Hopper, P. K. J Bioact Compat Polym 1995, 5, 453.
8. Dattaa, R.; Tsaia, S.-P.; Bonsignorea, P.; Moona, S.-H.; Frank, J. R. FEMS Microbiol Rev 1995, 16, 221.
9. Drumright, R. E.; Gruber, P. R.; Henton, D. E. Adv Mater 2000, 12, 1841.
10. Perepelkin, K. E. Fibre Chem 2002, 34, 85.
11. Snook, J. B. Biodegradation of Polylactide Film in Simulated Composting Environments; Michigan State University: East Lansing, MI, 1994; p 130.
12. Whiteman, N. Proceedings of the 2000 Polymers, Laminations and Coatings Conference, Chicago, IL, Aug 2000; Vol. 2; TAPPI Press: Atlanta, GA, p 631.
13. Gruber, P. R.; Hall, E. S.; Kolstad, J. H.; Iwen, M. L.; Benson, R. D.; Borchardt, R. L. U.S. Pat. 5,142,023 (1992).
14. Hartmann, M. H. In Biopolymers from Renewable Resources; Kaplan, D. L., Ed.; Springer-Verlag: Berlin, 1998; p 367.
15. Kharas, G. B.; Sanchez-Riera, F.; Severson, D. K. In Plastics from Microbes; Mobley, D. P., Ed.; Hanser: Munich, 1994; p 93.
16. Witzke, D. R. Introduction to Properties, Engineering, and Prospects of Polylactide Polymers; Michigan State University: East Lansing, MI, 1997; p 389.
17. Auras, R.; Harte, B.; Selke, S.; Hernandez, R. Proceedings of Worldpak 2002, East Lansing, MI; CRC Press: Boca Raton, FL, 2002; p 1011.
18. Conn, R. E.; Kolstad, J. J.; Borzelleca, J. F.; Dixler, D. S.; Filer, L. J., Jr.; LaDu, B. N.; Pariza, M. W. Food Chem Toxicol 1995, 33, 273.
19. Whiteman, N. Proceedings of Packexpo, Chicago, IL, Nov 2002; PMMI: Arlington, VA, p 37.
20. Baillie, J. Packag Week 1997, 13(22), 13.
21. Mohan, A. M. Packag Dig 2002, July 30.
22. Nageroni, J. Flexible Packag 2001, December 25.
23. O'Brien, M. Cargill Dow LLC Press Release, April 2, 2002. http://www.cargilldow.com/corporate/release.asp?id=95(Feb. 27, 2003).
24. O'Brien, M. Cargill Dow LLC Press Release, October 13, 2003. http://www.cargilldow.com/corporate/release.asp?id=124(Nov. 1, 2003).
25. O'Brien, M. Cargill Dow LLC Press Release, March 1, 2003. http://www.cargilldow.com/corporate/release.asp?id=112(Feb. 27, 2003).
26. Hernandez, R. J. J Food Eng 1994, 22, 495.
27. Gavara, R.; Hernandez, R. J. J Polym Sci Part B: Polym Phys 1994, 32, 2375.
28. Launay, A.; Thominette, F.; Verdu, J. J Appl Polym Sci 1999, 73, 1131.
29. Ravens, D. A. S.; Ward, I. M. Trans Faraday Soc 1960, 57, 150.
30. Auras, R.; Harte, B.; Selke, S. Annu Tech Conf Proc 2003, 3, 2862.
31. Michaels, A. S.; Vieth, W. R.; Barrie, J. A. J Appl Phys 1963, 34, 13.
32. Michaels, A. S.; Vieth, W. R.; Barrie, J. A. J Appl Phys 1963, 34, 1.
33. Polyakova, A.; Connor, D. M.; Collard, D. M.; Schiraldi, D. A.; Hiltner, A.; Baer, E. J Polym Sci Part B: Polym Phys 2001, 39, 1900.
34. Polyakova, A.; Liu, R. Y. F.; Schiraldi, D. A.; Hiltner, A.; Baer, E. J Polym Sci Part B: Polym Phys 2001, 39, 1889.
35. Gavara, R.; Hernandez, R. J. J Plast Film Sheeting 1993, 9, 126.
36. Crank, J. The Mathematics of Diffusion; Oxford University Press: London, 1975.
37. Chapra, S. C.; Canale, R. P. Numerical Methods for Engineers with Programming and Software Applications; McGraw-Hill: New York, 1998.
38. Hernandez-Munoz, P.; Gavara, R.; Hernandez, R. J. J Membr Sci 1998, 1.
39. Barr, C. D.; Giacin, J. R.; Hernandez, R. J. Packag Technol Sci 2000, 13, 157.
40. VanKrevelen, D. W. Properties of Polymers; Elsevier: Amsterdam, 1997.
41. Fischer, E. W.; Sterzel, H. J.; Wegner, G. Kolloid Z Z Polym 1973, 251, 980.
42. Wunderlich, B. Macromolecular Physics; Academic: New York, 1973.
43. Shigetomi, T.; Tsuzumi, H.; Toi, K.; Ito, T. J Appl Polym Sci 2000, 76, 67.
44. Sekelik, D. J.; Stepanov, E. V.; Nazarenko, S.; Schiraldi, D.; Hiltner, A.; Baer, E. J Polym Sci Part B: Polym Phys 1999, 37, 847.
45. Lewis, E. L. V.; Duckett, R. A.; Ward, I. M.; Fairclough, J. P. A.; Ryan, A. J. Polymer 2003, 44, 1631.
46. Hernandez, R. J.; Selke, S. E. M.; Culter, J. D. Plastics Packaging; Hanser: Munich, 2000.
47. Shogren, R. J Environ Polym Degrad 1997, 5, 91.